

On the entanglement of electrostriction and non-linear piezoelectricity in non-centrosymmetric materials

L. Pedesseau, C. Katan, and J. Even

Citation: *Appl. Phys. Lett.* **100**, 031903 (2012); doi: 10.1063/1.3676666

View online: <http://dx.doi.org/10.1063/1.3676666>

View Table of Contents: <http://apl.aip.org/resource/1/APPLAB/v100/i3>

Published by the [American Institute of Physics](http://www.aip.org).

Related Articles

Stress-controlled Pb(Zr_{0.52}Ti_{0.48})O₃ thick films by thermal expansion mismatch between substrate and Pb(Zr_{0.52}Ti_{0.48})O₃ film

J. Appl. Phys. **110**, 124101 (2011)

Electric field controlled magnetization rotation in exchange biased antiferromagnetic/ferromagnetic/piezoelectric composites

Appl. Phys. Lett. **99**, 232502 (2011)

Enhanced piezoelectric response of BaTiO₃-KNbO₃ composites

Appl. Phys. Lett. **99**, 202902 (2011)

A coupled analysis of the piezoresponse force microscopy signals

Appl. Phys. Lett. **99**, 171913 (2011)

Correlation between dielectric properties and chemical composition of the tourmaline single crystals

Appl. Phys. Lett. **99**, 142906 (2011)

Additional information on *Appl. Phys. Lett.*

Journal Homepage: <http://apl.aip.org/>

Journal Information: http://apl.aip.org/about/about_the_journal

Top downloads: http://apl.aip.org/features/most_downloaded

Information for Authors: <http://apl.aip.org/authors>

ADVERTISEMENT

The logo for AIP Advances features the text 'AIP Advances' in a blue and green font. Above the text is a decorative graphic of several orange and yellow circles of varying sizes, some connected by a dotted line, suggesting a path or a network.

Submit Now

Explore AIP's new
open-access journal

- Article-level metrics now available
- Join the conversation! Rate & comment on articles

On the entanglement of electrostriction and non-linear piezoelectricity in non-centrosymmetric materials

L. Pedesseau, C. Katan, and J. Even^{a)}

Université Européenne de Bretagne, France and FOTON, UMR 6082, INSA, F-35708 Rennes, France

(Received 17 November 2011; accepted 22 December 2011; published online 17 January 2012)

An extended and complete thermodynamical model of third-order electro-elastic coupling is proposed with symmetry analyses and density functional theory (DFT) calculations to evaluate consistently the various linear and non-linear coefficients. It is shown that in non-centrosymmetric materials, electrostrictive and non-linear piezoelectric phenomena are strongly coupled, except for materials crystallizing in a cubic lattice associated to the 432 point group. Thorough numerical results are given for GaN and AlN compounds in the Würtzite structure. Electrostriction dominates, but non-linear elasticity and non-linear piezoelectricity must be taken into account for strain evaluation whereas non-linear piezoelectricity yields a significant correction for electric field. © 2012 American Institute of Physics. [doi:10.1063/1.3676666]

Electrostrictive materials and generally materials which display large electromechanical interactions can be exploited in the areas of stress or displacement sensing and in actuating.^{1,2} It is also known that electrostrictive strains and large applied fields may cause breakdown of insulator materials used in small microelectronics devices. Non-linear elastic and piezoelectric effects in semiconductors have attracted attention in the last few years because highly strained materials are used intentionally to grow lattice mismatched nanostructures like quantum wells or quantum dots.³⁻⁷ The explanation of the observed first-order phase transition in ferroelectric materials like BaTiO₃ or SrTiO₃ requires the presence of suitable electrostrictive terms in the expression for the free energy of the material.^{8,9} Devonshire's theory relates the piezoelectric coefficients of the material in the polarized phase to the electrostrictive coefficients of the material in the unpolarized phase. In most experimental or theoretical works,¹⁰⁻¹⁴ nonlinearity in electrical, elastic, and electromechanical properties has been defined using formalisms related to Devonshire's theory. Yet, an extended and complete model of third-order electro-elastic coupling has been proposed in Ref. 14 using a systematic thermodynamical approach (Adam-Tichy-Kittinger model has been quoted ATK model in this paper).

Indeed, this letter aims to show that the ATK model can be combined systematically with symmetry analyses and DFT calculations to evaluate consistently the various linear and non-linear coefficients, especially in non-centrosymmetric materials. Symmetry properties of third-order elastic constants are well known^{15,16} but have been extensively studied for third-order coupled constants only more recently.^{17,18} The methods of density-functional perturbation theory (DPFT) may be used to calculate various physical responses. In fact, the efficient use of the "2n+1" theorem,²⁰ using only by-products of a first-order perturbation calculation,¹⁹⁻²¹ allows in principle to obtain the second and third-order derivatives of the total energy at the level of the ATK model, when the atomic-displacement variables are eliminated. Second-order derivatives of the total energy may be used with an existing

DPFT implementation²² to calculate various physical response properties of insulating crystals. Third-order derivatives are related to a number of physical properties described in this work, like the electrostrictive effects. However, most practical implementations of the DPFT are restricted to some quantities related to internal atomic displacements. In this paper, third-order coefficients are mostly determined from finite difference studies of materials polarisation or stress tensor under various electrical or strain conditions.

Here, we introduce thermodynamic potentials using standard definitions^{23,24} for the free enthalpy $G = U - \sigma_i \eta_i - TS$, the transformed free enthalpy $G_e = U - \sigma_i \eta_i - TS - E_l D_l$, and free energy $F_e = U - TS - E_l D_l$. The D_l , E_l vectors and the η_i , σ_i strain-stress tensors (in Voigt notation) are associated, respectively, to the l, m, n, u, v, o and i, j, k, p, q, r indices varying between 1-3 and 1-6. Three second-orders are defined for each of the thermodynamic potentials

$$\begin{aligned} d\sigma_i &= C_{ij}^E d\eta_j - e_{il} dE_l \text{ and } dD_l = e_{li} d\eta_i + \varepsilon_{lm}^{\eta} dE_m \text{ for } F_e, \\ d\eta_i &= S_{ij}^E d\sigma_j + d_{il} dE_l \text{ and } dD_l = d_{li} d\sigma_i + \varepsilon_{lm}^{\sigma} dE_m \text{ for } G_e, \\ d\eta_i &= S_{ij}^D d\sigma_j + g_{il} dD_l \text{ and } dE_l = -g_{li} d\sigma_i + \beta_{lm}^{\sigma} dD_m \text{ for } G. \end{aligned}$$

The second-order derivatives of the thermodynamic potentials are related to each others by exact relations^{23,24} like $\varepsilon_{lm}^{\sigma} - \varepsilon_{lm}^{\eta} = e_{lj} S_{ji}^E e_{im}$, $e_{il} = C_{ij}^E d_{jl}$, $S_{ij}^E - S_{ij}^D = g_{il} d_{lj}$. Four third-order derivatives are defined for F_e , G_e , and G

$$\begin{aligned} dC_{ij}^E &= C_{ijk}^E d\eta_k - B_{ijl} dE_l, de_{li} = B_{lij} d\eta_j + L_{lim} dE_m, \text{ and } d\varepsilon_{lm}^{\eta} \\ &= L_{lmi} d\eta_i + \varepsilon_{lmn}^{\eta} dE_n, \\ dS_{ij}^E &= S_{ijk}^E d\sigma_k + F_{ijl} dE_l, dd_{li} = F_{lij} d\sigma_j + M_{lim} dE_m, \text{ and } d\varepsilon_{lm}^{\sigma} \\ &= M_{lmi} d\sigma_i + \varepsilon_{lmn}^{\sigma} dE_n, \\ dS_{ij}^D &= S_{ijk}^D d\sigma_k + R_{ijl} dD_l, dg_{li} = R_{lij} d\sigma_j + Q_{lim} dD_m, \text{ and } d\beta_{lm}^{\sigma} \\ &= -Q_{lmi} d\sigma_i + \beta_{lmn}^{\sigma} dD_n. \end{aligned}$$

Most of these quantities are already used in various papers, but we will focus on the non-linear piezoelectric

^{a)} Author to whom correspondence should be addressed. Electronic mail: jacky.even@insa-rennes.fr.

tensors B_{lij} (Refs. 3–7, 17, and 18) and F_{lij} , R_{lij} (Refs. 17 and 18) and the electrostrictive tensors L_{lmi} ,¹⁷ M_{lmi} , and Q_{lmi} .^{8–13} The third-order derivatives of the thermodynamic potentials are also related to each other by various exact relations (adapted from ATK model)

$$F_{lij} = S_{ik}^E B_{lkp} S_{pj}^E + e_{lk} S_{kij}^E$$

and

$$R_{lij} = \beta_{lm}^\sigma F_{mij} - \beta_{lm}^\sigma \beta_{nv}^\sigma (M_{mni} d_{vj} + M_{mnj} d_{vi}) - \beta_{lmn}^\sigma d_{mi} d_{nj},$$

$$Q_{lmi} = \beta_{lmn}^\sigma d_{ni} + \beta_{mn}^\sigma \beta_{lv}^\sigma M_{vni} \text{ and}$$

$$M_{lmi} = (B_{lkp} d_{mp} + B_{mkp} d_{lp}) S_{ki}^E + L_{lmj} S_{ji}^E + e_{lk} e_{mj} S_{kji}^E.$$

These relations show that the tensors can be strongly entangled. Coefficients defined for a specific thermodynamical potential cannot be mixed with others in the same theoretical model without caution. For example, in the case of non-centrosymmetric materials, an additional term related to the linear piezoelectricity and the non-linear susceptibility must be added to the commonly used relation $Q_{lmi} = \beta_{mn}^\sigma \beta_{lv}^\sigma M_{vni}$.¹¹ Experimental determination of piezoelectric and electrostrictive entangled components must also rely on careful definitions of experimental conditions which makes such measurements very involved.¹¹ The direction of the applied field and the frequency behaviour are useful tools to separate the strains arising from piezoelectricity and electrostriction.

It is necessary to use symmetry properties of the materials in order to check whether or not the entanglement has to be taken into account. In order to get a first insight into the influence of lattice symmetry, we may compare materials which crystallise in a cubic lattice associated either to the m3m (e.g., diamond or undistorted perovskite lattices) and 432 point groups. In both cases, the linear piezoelectric tensors and non-linear susceptibilities are vanishing. Only six independent non-linear elastic constants and compliances exist.^{14,15} Q_{lmi} , M_{lmi} , and L_{lmi} tensors related to electrostriction are simply related, like in isotropic materials: $Q_{lmi} = \beta_{mn}^\sigma \beta_{lv}^\sigma M_{vni}$ and $M_{lmi} = L_{lmj} S_{ji}^E$, although the number of independent coefficients is larger. The only difference between the m3m and 432 point groups comes from the non-linear piezoelectricity phenomenon which appears only in the 432 case. Among the 32 crystal classes, 11 are centrosymmetric (m3m case) and 21 are non-centrosymmetric, but of these, 432 is a special case. For point group 432, non-linear piezoelectricity and electrostriction are indeed disentangled, and only one independent component B_{124} has to be determined: $F_{124} = (S_{11}^E - S_{12}^E) B_{124} S_{44}^E = \varepsilon^\sigma R_{124}$. However, in order to experimentally or theoretically study non-linear piezoelectric phenomenon from the polarization, the crystal must be strained simultaneously in a non-hydrostatic and shear strain state, as seen from the expression of the electric polarization (within cartesian coordinates and using Voigt notation for strain) $P = B_{124}((\eta_2 - \eta_3)\eta_4, (\eta_3 - \eta_1)\eta_5, (\eta_1 - \eta_2)\eta_6)$.

The case of the non-centrosymmetric $\bar{4}3m$ point group is more complex but corresponds to a large number of semiconductor materials of technological interest crystallizing in the zinc-blende lattice.^{3–5} Linear piezoelectric tensors and

non-linear susceptibilities correspond only to one non-zero component. Non-linear piezoelectric tensor has three independent components: B_{114} , B_{124} , B_{156} .^{3,4,17,18} The relations between B_{lij} , F_{lij} , and R_{lij} are more complex than for the 432 point group as illustrated by $F_{156} = S_{44}^E B_{156} S_{44}^E + e_{14} S_{456}^E$. Only one of the three independent electrostrictive components Q_{lmi} contains an additional contribution: $Q_{234} = \beta_{123}^\sigma d_{14} + \beta^\sigma \beta^\sigma M_{234}$. The electrostrictive and non-linear piezoelectric tensors, respectively, M_{lmi} and B_{lij} , are no longer independent as illustrated by $M_{111} = d_{14}(2B_{114} S_{11}^E + 4B_{124} S_{12}^E) + L_{111} S_{11}^E + 2L_{112} S_{12}^E + e_{14} e_{14} S_{144}^E$.

Among the hexagonal piezoelectric crystal classes, the 622 class is the most simple (e.g., beta quartz crystallographic structure). Only one linear and three non-linear piezoelectric components have to be defined.^{17,18} In this case, for quantum nanostructures with axial symmetry geometries, it is possible to use a cylindrical representation (r , φ , z) in linear elasticity.^{4,5,25} The components of the strain tensor depend only on four quantities $\varepsilon_{rr}(r, z)$, $\varepsilon_{\varphi\varphi}(r, z)$, $\varepsilon_{zz}(r, z)$, $\varepsilon_{rz}(r, z)$ and the piezoelectric polarization has only an

TABLE I. Electric and strain-related materials for AlN and GaN using DFT-LDA calculations via the ABINIT code.²² ε_{ij} and L_{ij} are the relative dielectric and electrostrictive tensors, respectively.

	AlN	GaN
a (Å)	3.060	3.219
c (Å)	4.898	5.244
c_{11} (GPa)	408	339
c_{12} (GPa)	138	133
c_{13} (GPa)	106	99
c_{33} (GPa)	380	375
c_{111} (GPa)	-1525	-1225
c_{112} (GPa)	-374	-834
c_{113} (GPa)	-66	-283
c_{123} (GPa)	-688	-631
c_{133} (GPa)	-1117	-967
c_{222} (GPa)	-271	-974
c_{333} (GPa)	-56	-1126
L_{11}	11.9	23.3
L_{12}	8.9	9.8
L_{13}	7.3	11.2
L_{31}	37.4	27.6
L_{33}	-73.6	-84.4
L_{44}	3.6	9.9
ε_{11}	5.3	7.0
ε_{33}	5.5	7.0
ε_{113} (10^{-12} m/V)	212	285
ε_{333} (10^{-12} m/V)	~0	985
ε_{3333} (10^{-18} m/V)	-17.6	-0.9
e_{31} (C/m ²)	-0.67	-0.41
e_{33} (C/m ²)	1.67	0.76
e_{15} (C/m ²)	-0.35	-0.29
B_{311} (C/m ²)	3.77	6.26
B_{312} (C/m ²)	4.12	2.37
B_{313} (C/m ²)	-8.64	-1.47
B_{333} (C/m ²)	-25.60	-23.43
B_{115} (C/m ²)	8.69	6.48
B_{125} (C/m ²)	5.19	5.09
B_{135} (C/m ²)	3.20	7.02
B_{344} (C/m ²)	2.88	1.41
P_{sp} (C/m ²)	-0.075	-0.014

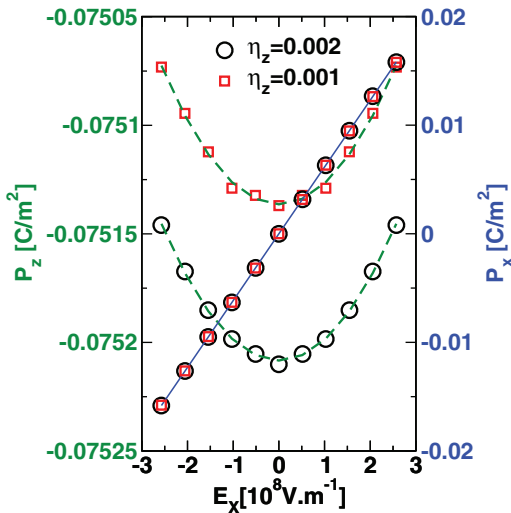


FIG. 1. (Color online) Variations of P_x and P_z as a function of E_x for AlN and various strain states along oz . The zero field and zero strain values of P_z are related to the spontaneous polarization, while the quadratic variation of P_z is related to the non-linear dielectric susceptibility.

angular component in cylindrical coordinates: $P_\theta = -2\epsilon_{rz}(e_{14} + B_{124}\epsilon_{rr} + B_{124}\epsilon_{\theta\theta} + B_{134}\epsilon_{zz})$. It is then straightforward to show that the internal electric field vanishes. For the electrostrictive tensor, $Q_{234} = \beta_{123}^\sigma d_{14} + \beta^\sigma \beta^\sigma M_{234}$.

Ten of the non-centrosymmetric crystal classes represent the polar crystal classes, which show a spontaneous polarization. For all this crystal classes, the entanglement of non-linear piezoelectricity and electrostriction is very strong. The hexagonal 6mm polar crystal class corresponds to a number of important materials in the wurtzite structure.^{6,7,12,26,27} We applied various electrical or strain conditions for the DFT determination of the coefficients in the case of the GaN and AlN crystals (Table I). Briefly, DFT simulations were performed through the *ab initio* open source ABINIT computer package²² within the local density approximation (LDA).²⁸ Plane wave basis sets were used with a kinetic energy cutoff of 950 eV after convergence studies. The sets of k-points were generated following the procedure of Pack and Monkhorst²⁸⁻³⁰ namely $10 \times 10 \times 10$. The pseudo potentials were generated for Ga [$3d^{10}4s^24p^1$] atom via the OPIUM code^{31,32} and for Al [$3s^23p^1$] and N [$2s^22p^3$] atoms via the FHI98PP code.³³ In Figure 1, the variations of P_x and P_z are reported for AlN and different strain states, as a function of E_x . The zero field and zero strain magnitude of P_z is related to the spontaneous polarization while the quadratic variation of P_z is related to the non-linear dielectric susceptibility. For GaN, the higher order electric (Kerr) effect dominates (Table I). The values of the cell parameters or linear coefficients are similar to those previously reported in the literature. If we consider a pure biaxial strain state perpendicular to the usual growth direction for nitride heterostructures (oz), the polarisation has only one component $P_z = P_{sp} + e_{33}\epsilon_\perp + 2e_{31}\epsilon_{//} + (B_{311} + B_{312})e_{//}^2 + \frac{B_{333}}{2}\epsilon_\perp^2 + 2B_{313}\epsilon_{//}\epsilon_\perp$. In the corresponding relation given in Ref. 7, indices are interchanged but, more importantly, incorrect numerical prefactors and one of the eight tensor components namely B_{312} are lacking. Given these corrections, both DFT studies give similar numerical values, except for the

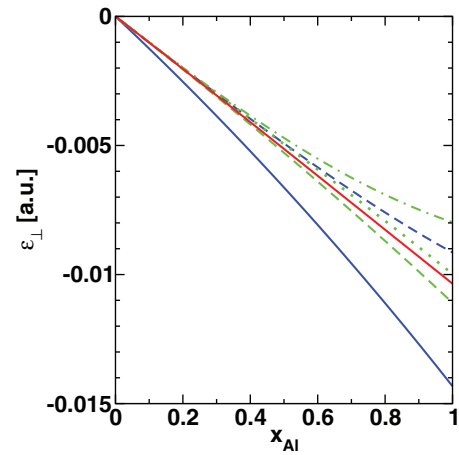


FIG. 2. (Color online) Variation of ϵ_\perp as a function of Al mole fraction for various models. The results of the uncoupled and coupled linear models are represented by straight and dashed blue lines (the first (bottom) and the fifth curves), the coupling etc. The straight red line (third curve) includes all the non-linear contributions. The electrostrictive, the non-linear elastic and the non-linear piezoelectric ones are represented by dashed (second curve), dashed/dotted (sixth curve), and dotted green lines (fourth curve).

B_{313} that remains in both cases much more important for AlN than GaN. The electromechanical coupling can be studied in AlGaN/GaN heterojunctions²⁷ including all the non-linear effects. Figure 2 shows the variation of ϵ_\perp as a function of Al mole fraction for various models. The coupling strongly reduces ϵ_\perp in linear models. It is, however, overestimated as shown by the straight red line including all the non-linear contributions. Among these, the electrostrictive, the non-linear elastic and the non-linear piezoelectric ones are the most important (in decreasing order). The non-linear elastic contribution is opposite to the other ones. Variation of the electric field E_z , as a function of Al mole fraction, is reported in Figure 3 for various models. The coupling strongly enhances E_z in linear models. Once more, when including all the non-linear contributions, the electrostrictive

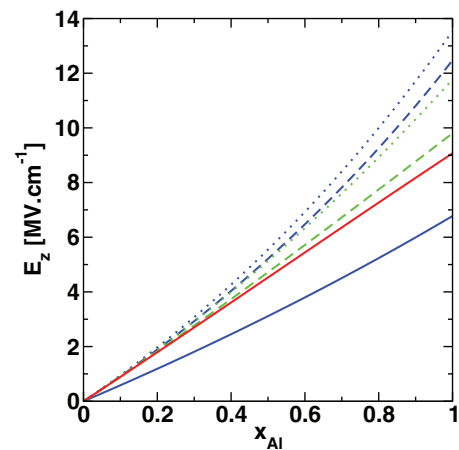


FIG. 3. (Color online) Variation of the electric field E_z as a function of Al mole fraction for various models. The results of the uncoupled and coupled linear models are represented by straight (first (bottom) curve) and dashed (fifth curve) blue lines, the coupling strongly enhancing E_z . The linear semi-coupled “standard” model,²⁷ is represented by a dotted blue line (sixth curve). The straight red line (second curve) includes all the non-linear contributions. The electrostrictive and the non-linear piezoelectric ones are represented by dashed (third curve) and dotted (fourth curve) green lines.

contribution dominates and reduces the effect of coupling (Figure 3). Using relation $M_{lmi} = (B_{lkp}d_{mp} + B_{mkp}d_{lp})S_{ki}^E + L_{lmi}S_{ji}^E + e_{lk}e_{mj}S_{kji}^E$, it is shown that whatever the Al mole fraction, the most important contribution to M_{33} is due to L_{lmi} but non-linear piezoelectric effect can no longer be ignored. M_{33} calculated for GaN ($2.8 \times 10^{-21} \text{ m}^2 \text{ V}^{-2}$) is rather large¹¹ but much smaller than the record experimental value of $1.8 \times 10^{-18} \text{ m}^2 \text{ V}^{-2}$ reported in Ref. 12. This experimental result has, however, not yet been confirmed, neither for GaN nor for any other semiconductor compounds. We may underline that in this field, incomplete formula for the M_{lmi} tensor have been used up to now.^{6,34,35}

An extended and self-contained thermodynamical model of third-order electro-elastic coupling is used with symmetry analyses and DFT calculations to evaluate properly the various linear and non-linear coefficients. It is shown that in non-centrosymmetric materials, electrostrictive and non-linear piezoelectric phenomena are strongly coupled, except for materials crystallizing in a cubic lattice associated to point group 432. The whole simulations have been explored for GaN and AlN compounds in the Würtzite structure. For these materials, both phenomena must be taken into account simultaneously at the same level of theory or experiment. Electrostriction dominates, but non-linear elasticity and non-linear piezoelectricity must be taken into account for strain evaluation, whereas non-linear piezoelectricity yields a significant correction for electric field. Coupled linear models overestimate the corrections with respect to uncoupled linear ones and we recommend the use of full coupled non-linear models.

¹R. E. Pelrine, R. D. Kornbluh, and J. P. Joseph, *Sens. Actuators, A* **64**, 77 (1998).

²A. Wingert, M. D. Lichter, and S. Dubowsky, *IEEE/ASME Trans. Mechatron.* **11**, 448 (2006).

³G. Bester, X. Wu, D. Vanderbilt, and A. Zunger, *Phys. Rev. Lett.* **96**, 187602 (2006).

- ⁴J. Even, F. Doré, C. Cornet, L. Pédesseau, A. Schliwa, and D. Bimberg, *Appl. Phys. Lett.* **91**, 122112 (2007).
- ⁵J. Even, F. Doré, C. Cornet, and L. Pedesseau, *Phys. Rev. B* **77**, 085305 (2008).
- ⁶L. C. Lew Yan Voon and M. Willatzen, *J. Appl. Phys.* **109**, 031101 (2011).
- ⁷J. Pal, G. Tse, V. Haxha, and M. A. Migliorato, *Phys. Rev. B* **84**, 085211 (2011).
- ⁸A. F. Devonshire, *Adv. Phys.* **3**, 94 (1954).
- ⁹G. Rupprecht and D. Winter, *Phys. Rev.* **155**, 1019 (1967).
- ¹⁰Z. Y. Meng and L. E. Cross, *J. Appl. Phys.* **57**, 491 (1985).
- ¹¹R. E. Newnham, V. Sundar, R. Yimnirun, J. Su, and Q. M. Zhang, *J. Phys. Chem. B* **101**, 10141 (1997).
- ¹²I. L. Guy, S. Muensit, and E. M. Goldys, *Appl. Phys. Lett.* **75**, 3641 (1999).
- ¹³Y. Cho and K. Yamanouchi, *J. Appl. Phys.* **61**, 875 (1986).
- ¹⁴W. Adam, J. Tichy, and E. Kittinger, *J. Appl. Phys.* **64**, 2556 (1988).
- ¹⁵F. G. Fumi, *Phys. Rev.* **83**, 1274 (1951).
- ¹⁶K. Brugger, *J. Appl. Phys.* **36**, 759 (1965).
- ¹⁷D. Gerlich and M. A. Breazeale, *J. Appl. Phys.* **68**, 5119 (1990).
- ¹⁸H. Grimmer, *Acta Cryst. A* **63**, 441 (2007).
- ¹⁹S. Baroni, P. Gianozzi, and A. Testa, *Phys. Rev. Lett.* **59**, 2662 (1987).
- ²⁰X. Gonze and J. P. Vigneron, *Phys. Rev. B* **39**, 13120 (1989).
- ²¹D. R. Hamann, X. Wu, K. M. Rabe, and D. Vanderbilt, *Phys. Rev. B* **71**, 035117 (2005).
- ²²X. Gonze, B. Amadon, P.-M. Anglade, J.-M. Beuken, F. Bottin, P. Boulanger, F. Bruneval, D. Caliste, R. Caracas, M. Cote *et al.*, *Comput. Phys. Commun.* **180**, 2582 (2009).
- ²³J. F. Nye, *Physical Properties of Crystals: Their Representation by Tensors and Matrices* (Oxford University Press, New York, 1985).
- ²⁴E. Dieulesaint and D. Royer, *Ondes élastiques dans les solides – propagation libre et guidée* (Masson, Paris Milan Barcelone, 1996).
- ²⁵J. Even, *Appl. Phys. Lett.* **94**, 102105 (2009).
- ²⁶I. Vurgaftman and J. R. Meyer, *J. Appl. Phys.* **94**, 3675 (2003).
- ²⁷B. Jogai, J. D. Albrecht, and E. Pan, *J. Appl. Phys.* **94**, 3984 (2003).
- ²⁸J. P. Perdew and Y. Wang, *Phys. Rev. B* **45**, 13244 (1992).
- ²⁹H. J. Monkhorst and J. D. Pack, *Phys. Rev. B* **13**, 5188 (1976).
- ³⁰J. D. Pack and H. J. Monkhorst, *Phys. Rev. B* **16**, 1748 (1977).
- ³¹G. G. P. Licence, Opium code version 3.6 (October 2010), <http://opium.sourceforge.net>.
- ³²I. Grinberg, N. Ramer, and A. Rappe, *Phys. Rev. B* **62**, 2311 (2000).
- ³³M. Fuchs and M. Scheffler, *Comput. Phys. Commun.* **119**, 67 (1999).
- ³⁴M. Bahrami-Samani, S. R. Patil, and R. Melnik, *J. Phys.: Condens. Matter* **22**, 495301 (2010).
- ³⁵I. Kornev, M. Willatzen, B. Lassen, and L. C. Lew Yan Voon, *AIP Conf. Proc.* **1199**, 71 (2010).